LED-pumped Er:Cr:YSGG light sources

Lisa Lopez, Frédéric Druon, Patrick Georges, François Balembois

Research Article | Vol. 31, No. 17 / 14 Aug 2023 / Optics Express 27604
Optics EXPRESS

LED-pumped Er:Cr:YSGG light sources

LISA LOPEZ,* FRÉDÉRIC DRUON, PATRICK GEORGES, AND FRANÇOIS BALEMBOIS

Université Paris-Saclay, Institut d'Optique Graduate School, Centre National de la Recherche Scientifique, Laboratoire Charles Fabry, 91127, Palaiseau, France
*lisa.lopez@institutoptique.fr

Abstract: For, what we believe is, the first time, an Er:Cr:YSGG crystal is pumped by LEDs through a Ce:YAG luminescent concentrator. We demonstrate both laser emission at 2.79 µm and strong spontaneous emission at 1.6 µm. The luminescent concentrator delivers 1.5 ms pulses at 10 Hz in the visible (550-650 nm) to the Er:Cr:YSGG crystal, in a transverse pumping configuration. The Er:Cr:YSGG laser produces up to 6.8 mJ at 2.79 µm in a biconcave cavity. The Er:Cr:YSGG also stands out as a bright broadband incoherent source around 1.6 µm with a unique combination of peak power (351 mW) and brightness (1.4 W/sr/cm^2).

1. Introduction

Er:Cr:YSGG (erbium, chromium doped yttrium scandium gallium garnet) is a well-known crystal with laser emission at 2.79 µm [1], useful for medical applications, in particular for dental surgery to cut soft tissue, bone, enamel and dentin [2,3] or to increase the surface hardness of dentin [4]. The energy transfer between Cr and Er allows this crystal to be pumped with flashlamps emitting mainly in the visible spectral band. While many papers report investigations of Er:Yb:YSGG studies on various dental treatments, very few results are devoted to the development of this laser [5,6]. Research is more focused on diode-pumping of Er:YSGG around 970 nm [7–9]. In fact, diode-pumping offers a better efficiency and the possibility to work on a small spot at a high repetition rate (kHz). In dentistry, this is suitable for the selective removal of calculus [10] or caries [11]. Although the efficiency of flashlamp-pumped laser systems is very low compared to diode-pumped systems, flashlamps can deliver a high amount of energy at low cost for hundreds of microseconds, which could be advantageous for rapid cutting or ablation. This certainly explains why flashlamp Er:Cr:YSGG lasers are still widely used despite the age of flashlamp technology. The maturity of this technology is clearly an important advantage, but it is still interesting to explore alternative innovative technologies for pumping Er:Cr:YSGG.

With the recent development of LED, new opportunities for laser pumping are emerging, especially with near-infrared LEDs adapted for pumping Nd-doped lasers [12–14]. Considering the absorption spectrum of Er:Cr:YSGG (Fig. 1), blue LEDs seem to be more suitable than near-infrared LEDs. Direct pumping with blue LEDs has been investigated in [15] with a co-doped Ce:Nd:YAG and could also be a solution for pumping the Er:Cr:YSGG. However, in this configuration, the number of LEDs is limited by the size of the laser crystal and the size of the pumping chamber. In addition, the pump power density is less than 100 W/cm^2, which makes it difficult to reach the oscillation threshold. For these reasons, we prefer to implement indirect LED pumping using a Ce:YAG luminescent concentrator pumped by blue LEDs [16].

This configuration allows a massive collection of LEDs and delivers a pump beam in the range of 1-10 kW/cm^2 in the yellow-orange spectral band. LED-pumped Ce:YAG concentrators have been used as pumped sources for lasers such as Nd:YVO_4 [16], alexandrite [17], Ti:sapphire [18], and Cr:LiSAF [19]. At the output of the Ce:YAG luminescent concentrator, the available pump energy can reach 270 mJ for a pulse duration of 260 µs at a repetition rate of 10 Hz [17]. So far, such lasers LED-pumped by luminescent concentrators have been only investigated in the

#496359 https://doi.org/10.1364/OE.496359
Journal © 2023 Received 25 May 2023; revised 24 Jun 2023; accepted 30 Jun 2023; published 2 Aug 2023

Optics EXPRESS

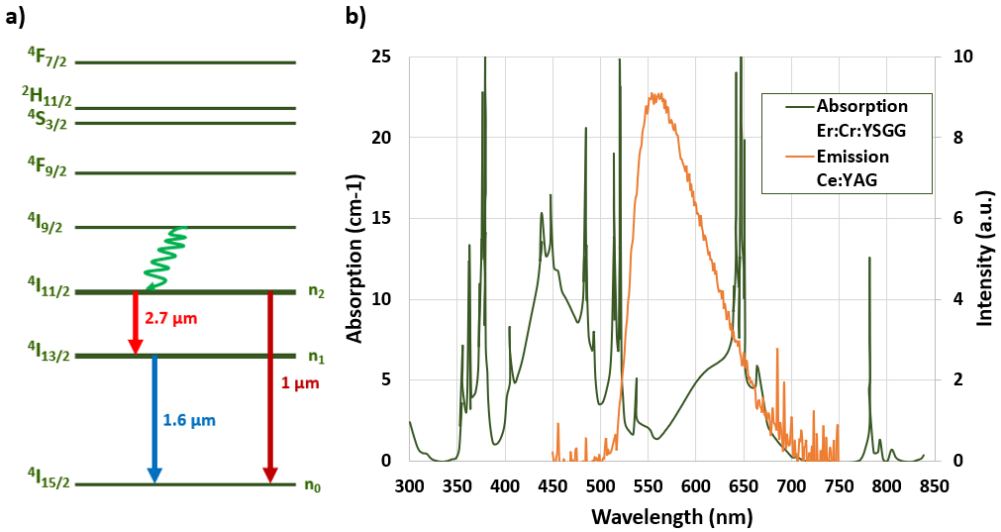

Fig. 1. a) Energy level diagram for the trivalent erbium ion. The $^4I_{9/2}$ level is populated by energy transfer from $^4A_2$ of the Cr^{3+} ion. b) Emission spectra of Ce:YAG (orange) and Er:Cr:YSGG absorption coefficient (green).

near infrared. We propose, for the first time, to extend this technology to longer wavelengths of interest. In this paper, we investigate LED-pumping of Er:Cr:YSGG using a Ce:YAG luminescent concentrator. The entire emission spectrum of Er:Cr:YSGG is studied : at 2.79 µm we explore laser operation by inserting the crystal into a two-mirror cavity. At 1 µm and 1.6 µm, we study the broadband spontaneous emission emitted by the Er:Cr:YSGG crystal considered as a second luminescent concentrator in a cascade configuration.

2. LED-pumped laser

2.1. Experimental setup

The crystal used in this study is an Er:Cr:YSGG (from Crylink) with dimensions of 3×1x14 mm^3 polished on all faces. Its concentration is 30 at.% for erbium ions (3.7×10^{21} cm^{-3}, Er^{3+} in dodecahedral site) and 2 at.% for chromium ions (1.7×10^{20} cm^{-3}, Cr^{3+} in octahedral site). The Er^{3+} concentration is optimized for laser emission around 2.7 µm. Indeed, laser operation at the $^4I_{11/2} \rightarrow {}^4I_{13/2}$ transition (Fig.1a) is limited by the self-terminating "bottleneck" effect since the lifetime of the upper laser level is shorter than that of the lower level. However, this effect can be mitigated by energy transfer upconversion occurring at the $^4I_{13/2}$ level. This effect is favored by increasing the doping concentration of Er^{3+} (>30 at.%) [20].

As pump source, we chose a Ce:YAG luminescent concentrator pumped by blue LEDs. Fig.1b shows the spectral overlap between the Ce:YAG emission and the Er:Cr:YSGG absorption, mainly due to Cr^{3+} ions. Under experimental conditions (Fig. 2), we measured an absorption of 57%. with an integrating sphere. It is worth noting that it is much higher than the absorption of 1 mm thick Er:Cr:YSGG. In fact, the light entering the Er:Cr:YSGG is Lambertian, so the average path in the concentrator is much higher than the crystal thickness. In addition, since Ce:YAG and Er:Cr:YSGG are bonded together (Fig. 2), some of the light transmitted through the Ce:YAG cannot escape into the air and is therefore trapped by total internal reflection on the faces of the Er:Cr:YSGG.

Optics EXPRESS

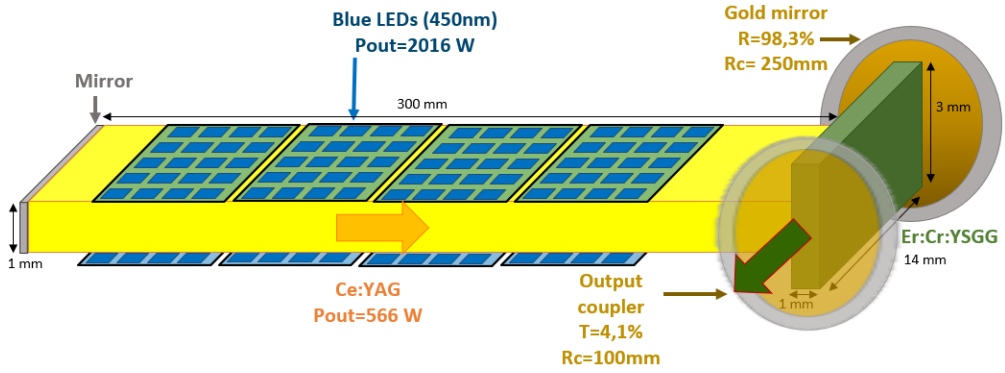

Fig. 2. Experimental setup of the Er:Cr:YSGG laser at 2.79 µm pumped by blue LEDs via a Ce:YAG luminescent concentrator. The total peak power of the blue LEDs and the peak power of Ce:YAG launched in the Er:Cr:YSGG are indicated.

The blue LEDs have an emission spectrum centered at 450 nm (LUXEON Z Royal Blue from Lumileds). At a drive current of 1 A, each LED emits 900 mW over an area of 1×1 mm^2. To avoid strong thermal effects, the LEDs operate in a quasi-continuous wave at 10 Hz with a pulse duration of 1.5 ms, close to the $^4I_{11/2}$ lifetime of Er:Cr:YSGG (1.4 ms [1]). We use 2240 LEDs arranged in two panels of 1120 LEDs each with dimensions of 14×200 mm^2. The concentrator consists of three $1 \times 14 \times 100$ mm^2 Ce:YAG (from Crytur) polished on all sides and glued together by UV curing to form a $1 \times 14 \times 300$ mm^2 plate. Due to the refractive index difference between the adhesive (n = 1.48) and the YAG (n = 1.82), the Fresnel losses at each interface are only 1%. This 300-mm-long slab is chosen for space reasons between the mechanics of the pump head and the mounts of the cavity mirrors. The large faces of the concentrator are pumped by the LED panels (Fig. 2). The thickness of the concentrator (1 mm) is sufficient to absorb all the blue light from the LEDs and to ensure good mechanical handling of the assembly. A metal mirror is placed on one of the 1×14mm^2 edges to collect more energy. The other 1×14mm^2 edge is considered the output side. When the LEDs are driven at 1A (10 Hz 1.5 ms), we measure an energy of 324 mJ resulting in an LED/concentrator efficiency of 11%. (Joule meter ref ES120C from Thorlabs).

The Er:Cr:YSGG is bonded to the Ce:YAG at the center of its large area (14×3 mm^2) with UV-curing optical adhesive. Considering the refractive index of the adhesive (n = 1.48), the internal total reflection angle in Ce:YAG is increased from 33° (in air) to 54° (in adhesive). Therefore, the energy coupled in the adhesive and thus in the Er:Cr:YSGG is more important than the output energy in air. Taking into account the Fresnel reflections at the various interfaces, we estimate the energy coupled into the Er:Cr:YSGG to be 850 mJ. At a repetition rate of 10 Hz, the average power absorbed reaches 4 W. The crystal is simply cooled with pulsed air.

The cavity consists of two concave mirrors: a gold mirror (reflectivity of 98.3%) and an output coupler as output mirror (transmission of 4.1% at 2785 nm). The radius of curvature are 250 mm and 100 mm, respectively. The cavity length is reduced to 24 mm to limit losses due to water absorption in air which are significant at 2.79 µm (typically 5 m^{-1} at 2.79 µm corresponding to losses of 10% on a round trip in the cavity).

2.2. *Performance*

Figure 3(a) shows the pump signal (Ce:YAG) and the laser signal. Since the lifetime of Ce:YAG is 70 ns, the pump signal can be considered as a square on the 100 µs scale. The laser starts 40 µs after power-on. It exhibits many spikes characteristic of a free-running laser with a gain medium whose upper state lifetime is much longer than the laser cavity lifetime. The laser decays after the

Optics EXPRESS

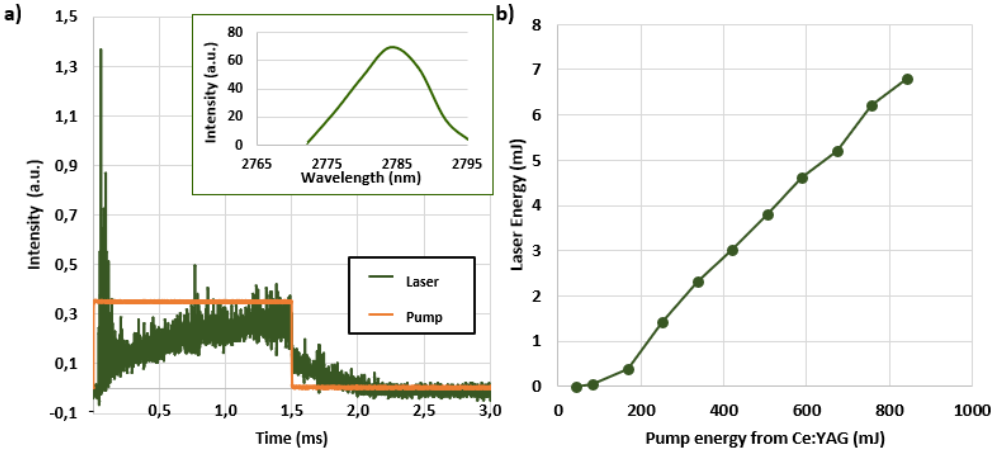

Fig. 3. a) Laser and pump temporal profile. Inset: laser spectrum b) Laser output energy versus luminescent concentrator pumping energy.

end of pumping, in accordance with the long upper-state lifetime of the $^4I_{11/2}$ level(1.4 ms [1]). The measured spectrum is centered at 2785 nm with a spectral width of 20 nm (inset Fig.3a). The laser output energy is plotted as a function of the pump energy from the luminescent concentrator in Fig.3b. A maximum laser energy of 6.8 mJ is obtained. The optical efficiency is then 0.8% with respect to the optical energy launched in the Er:Cr:YSGG crystal. This efficiency is similar to the one of a flash-pumped Er:Cr:YSGG laser [1]. Even without mirrors, we observe laser oscillations on the output faces of the Er:Cr:YSGG that are not antireflection coated. Given the refractive index of the crystal (n = 1.92), the small signal gain is then greater to 10 per single pass at the maximum pump energy. In the cavity, the losses induced by the two mirrors are only 6% per round trip and as the cavity is very small the water absorption is low. This explains why the oscillation threshold in the two-mirror cavity is so low.

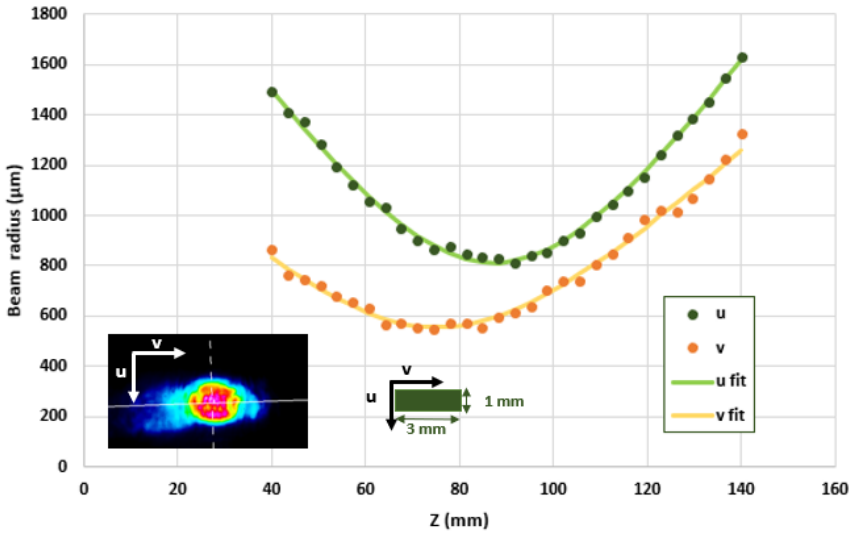

Fig. 4. Beam quality measurement (M^2) of the laser beam at 2785 nm at maximum pump energy. Insert: spatial profile of the laser at the focus point.

Optics EXPRESS

The measured beam profile (with the MIR camera WinCamD-IR-BB from DataRay) shows a spatially multimode laser (Fig. 4 inset). Indeed, the transverse pumping configuration together with a low absorption provides a gain volume much larger than the fundamental gaussian mode of the cavity (103×267 µm^2). The output laser beam has a spatial quality factor M^2 of 6 in the largest dimension of the output face and 3 in the other dimension, as shown in Fig. 4. In fact, the small size (1 mm) in this dimension acts as an aperture filter.

3. Er:Cr:YSGG as a luminescent concentrator

By scanning the emission of our Er:Cr:YSGG crystal with a spectrometer, we observe a strong fluorescence signal at 1 µm and at 1.6 µm, corresponding to the $^4I_{11/2} \rightarrow {}^4I_{15/2}$ transition and to the $^4I_{13/2} \rightarrow {}^4I_{15/2}$ transition respectively. Since our crystal is polished on all faces, it is convenient to use it as a luminescent concentrator, directing part of the spontaneous emission to the output face (1×3 mm^2). Therefore, we investigate the performance of Er:Cr:YSGG as a luminescent concentrator for a very broadband incoherent light emission in the SWIR (short-wave infrared usually between 0.9-1.7 µm) spectral band.

3.1. Experimental set up

The experimental setup of the LED-pumped luminescent concentrator is shown in Fig. 5. The setup is the same as previously except for the concave mirrors that have been replaced. Close to the back side, we put a plane mirror (mid-infrared enhanced gold mirror from Thorlabs) in order to recycle the rays emitted in the backward direction. On the output side, a compound parabolic concentrator (CPC #17-709 from Edmund) is glued (UV-curing) to improve the light extraction and to reduce the numerical aperture of the output beam as reported in a similar setup [21]. In our case, the numerical aperture is reduced to 0.6 and the output beam after the CPC has a diameter of 5 mm.

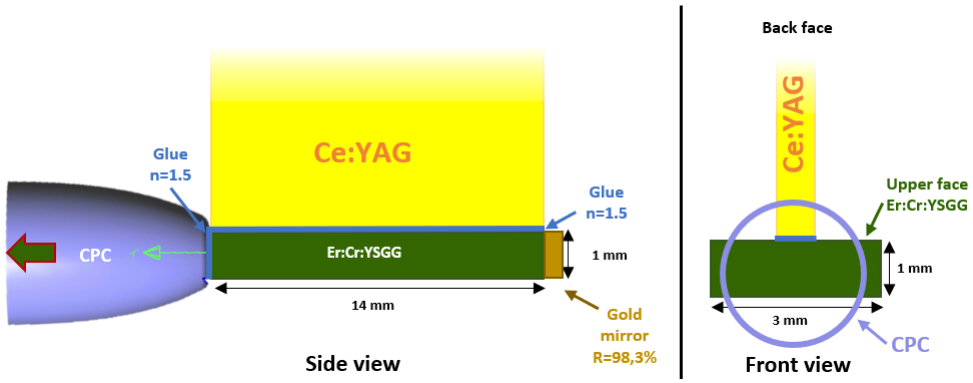

Fig. 5. Experimental set-up of the LED pumped Er:Cr:YSGG luminescent concentrator. CPC: compound parabolic concentrator

3.2. Results

At maximum pump energy, we still observe a parasitic laser effect at 2.79 µm between the output face of the CPC and the back mirror, corresponding to an energy of 540 µJ (detected after a germanium window suppressing the emission below 2 µm WG91050 from Thorlabs). This effect prevents us from exploiting the fluorescence around 2.7 µm. In addition, it reduces the population of the upper level $^4I_{11/2}$ and thus the efficiency of the 1 µm emission. However, it contributes to

Optics EXPRESS

the population of the $^4I_{13/2}$ level, in addition to other excitation pathways such as cross relaxation between the ground state and the $^4I_{9/2}$ level [1].

We start the characterization of the concentrator by measuring the output signal with a fast photodiode (PDAVJ8 from Thorlabs). The emission at 1.6 µm is selected with a bandpass filter (FB1750-50 from Thorlabs). Figure 6 shows the temporal profile of this emission. The decreasing part of the curve is compared to the fluorescence decay only considering the lifetime of $^4I_{13/2}$ (5.1 ms [1]). Figure 6 shows a strong difference between the two characteristic times, which can be related to the upconversion taking place at the $^4I_{13/2}$ level. This effect is indeed favored by the high Er doping level and clearly made to promote the 2.79 µm emission. However, its drawback is that it significantly reduces the emission at 1.6 µm.

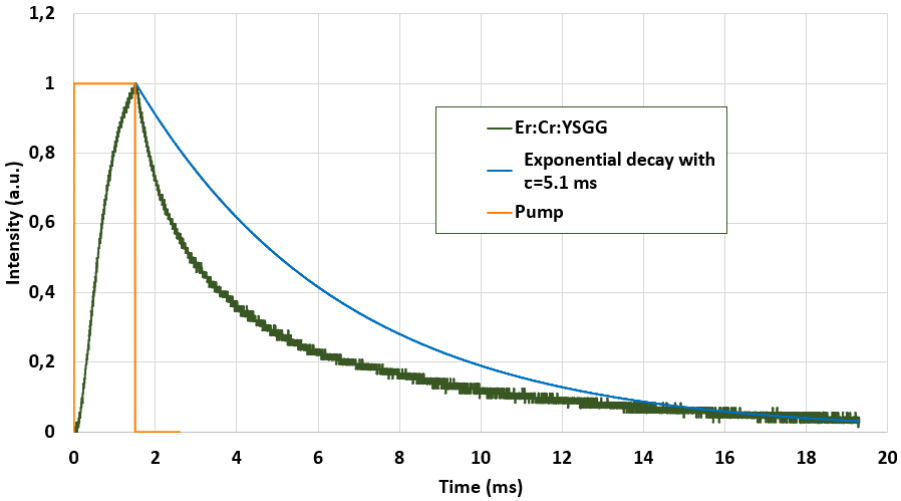

Fig. 6. Temporal shape of the emission at 1.6 µm. In dash line, fluorescence decrease assuming a single exponential decrease with a lifetime of 5.1 ms corresponding to the lifetime of the $^4I_{13/2}$.

An output energy of 900 µJ at 1.6 µm has been measured, using a pyroelectric energy sensor (ES120C from Thorlabs) in combination with the bandpass filter (FB 1750-500 from Thorlabs). This corresponds to an optical conversion efficiency of 0.1% for the Er:Cr:YSGG. To understand this low value, we estimate the propagation losses in the crystal. This is done by comparing the output power with and without the gold back mirror [22]. The loss coefficient is measured to be 0.77 cm^{-1} at 1.6 µm. These losses are related to the thermal population of the $^4I_{15/2}$ and the high erbium doping level (30%). Thus, the low efficiency has two main causes: upconversion, which reduces the excited state population, and reabsorption losses, which reduce the emission at 1.6 µm.

The temporal shape of the emission at 1.6 µm gives a peak power of 351 mW after the CPC. The output spectrum is measured (using NIRQuest from Ocean Insight) over the 0.9 µm to 2 µm band. The spectral luminance at the output of the CPC reaches 0.14 W/cm^2/sr/nm at 1.640 µm and 0.06 W/cm^2/sr/nm at 1.014 µm (Fig. 7).

To demonstrate the relevance of this Er:Cr:YSGG source of spontaneous emission, it is interesting to compare its performance with that of other sources emitting in the SWIR (Fig. 7). While the emission at 1 µm is not particularly relevant, the spectral luminance of the Er:Cr:YSGG at 1.6 µm is 50 times better than commercial LEDs and 15 times better than a black body at 1500 K. The spectral luminance remains far below that of an Er-doped fiber ASE source. However, its spectral-emission bandwidth -of 200 nm FWHM- is much wider. Therefore, the

Optics EXPRESS

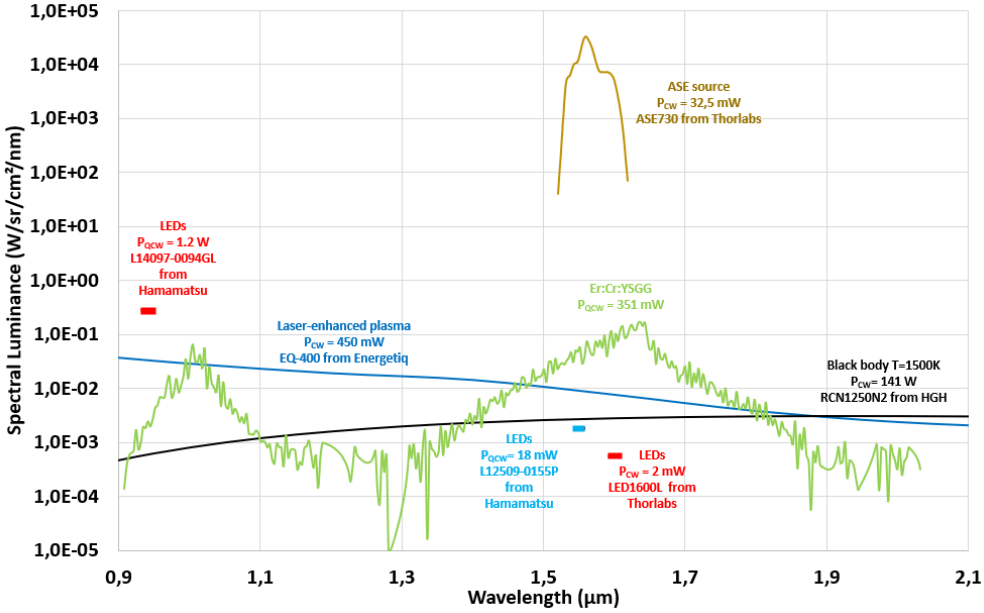

Fig. 7. State of the art of incoherent sources spectral luminance in the SWIR. P_{xxx} corresponds to the average powers for continuous sources and to the peak power for quasi-continuous sources.

Er:Cr:YSGG luminescent concentrator is a broadband SWIR source with a unique combination of power and brightness that is interesting for lighting applications.

4. Conclusion

This work presents the first laser emission of an LED-pumped Er:Cr:YSGG at 2.79 µm, producing 6.8 mJ pulses in free-running mode at 10 Hz. The output power can be further optimized by choosing a suitable output coupler or a more reflective dielectric back mirror, by antireflection coating of the crystal faces, and by designing a cavity with better overlap between the pump beam and the laser beam. This new laser represents an original proof of concept that LED-pumping is an interesting and promising technology for the development of SWIR laser sources, combining energy (10-100 mJ), repetition rate (100 Hz) and robustness thanks to the ultra-long lifetime of the LED.

This work also demonstrates for the first time that Er:Cr:YSGG can be used as a spontaneous emission source at 1.6 µm with unique properties. Its performance already exceeds that of classical incoherent SWIR sources such as LEDs and black bodies. In our experiment, the Er doping level (30%) was optimized for laser emission at 2.79 µm, but not for emission at 1.6 µm. A doping level of 5%, which is suitable for emission at 1.6 µm [20], could have greatly reduced the upconversion losses and the reabsorption losses. Therefore, there is considerable room for improvement for this new light source in the SWIR that could address applications such as night vision surveillance, optical communications, remote sensing, and biomedical imaging [23,24].

Funding. Agence Nationale de la Recherche (ANR-21-CE08-0044, project NewLight); Agence de l'innovation de Défense.

Disclosures. The authors declare no conflicts of interest.

Optics EXPRESS

Data Availability. Data underlying the results presented in this paper are not publicly available at this time but may be obtained from the authors upon reasonable request.

References

1. P. F. Moulton, J. G. Manni, and G. A. Rines, "Spectroscopic and laser characteristics of Er,Cr:YSGG," IEEE J. Quantum Electron. **24**(6), 960–973 (1988).
2. J. Diaci and B. Gaspirc, "Review : Comparison of Er:YAG and Er,Cr:YSGG lasers used in dentistry" Journal of the Laser and Health Academy Vol. 2012, No.1;
3. B. R. Masters, "Three-dimensional microscopic tomographic imaging of the cataract in a human lens in vivo," Opt. Express **3**(9), 332 (1998).
4. M. Hassan, E. Bakhurji, and R. AlSheikh, "Application of Er,Cr:YSGG laser versus photopolymerization after silver diamine fluoride in primary teeth," Sci. Rep. **11**(1), 20780 (2021).
5. F. Könz, M. Frenz, V. Romano, M. Forrer, H. P. Weber, A. V. Kharkovskiy, and S. I. Khomenko, "Active and passive Q-switching of a 2.79 µm Er: Cr: YSGG laser," Opt. Commun. **103**(5-6), 398–404 (1993).
6. P. Maak, L. Jakab, P. Richter, H. J. Eichler, and B. Liu, "Efficient acousto-optic Q switching of Er:YSGG lasers at 279-µm wavelength," Appl. Opt. **39**(18), 3053 (2000).
7. B. J. Dinerman and P. F. Moulton, "3-µm cw laser operations in erbium-doped YSGG, GGG, and YAG," Opt. Lett. **19**(15), 1143 (1994).
8. E. Arbabzadah, S. Chard, H. Amrania, C. Phillips, and M. Damzen, "Comparison of a diode pumped Er:YSGG and Er:YAG laser in the bounce geometry at the 3 µm cwx < qtransition," Opt. Express **19**(27), 25860 (2011).
9. H. Nie, Q. Hu, B. Zhang, X. Sun, H. Tian, Y. Wang, B. Yan, Z. Jia, K. Yang, X. Tao, and J. He, "Highly Efficient Continuous-Wave and Passively Q-Switching 2.8-µm Er:YSGG Laser," IEEE Photonics Technol. Lett. **30**(15), 1400–1403 (2018).
10. D. Fried, W. Fried, K. Chan, and C. Darling, "Selective removal of dental calculus with a diode-pumped Er:YAG laser,", SPIE – Lasers in Dentistry XXV, 2019), p. 21.
11. R. Yan, K. H. Chan, H. Tom, J. C. Simon, C. L. Darling, and D. Fried, "Selective removal of dental caries with a diode-pumped Er:YAG laser, " SPIE 9306 - Lasers in Dentistry XXI, (2015), p. 93060O.
12. A. Barbet, F. Balembois, A. Paul, J.-P. Blanchot, A.-L. Viotti, J. Sabater, F. Druon, and P. Georges, "Revisiting of LED pumped bulk laser: first demonstration of Nd:YVO_4 LED pumped laser," Opt. Lett. **39**(23), 6731 (2014).
13. K. Y. Huang, C. K. Su, M. W. Lin, Y. C. Chiu, and Y. C. Huang, "Efficient 750-nm LED-pumped Nd: YAG laser," Opt. Express **24**(11), 12043–12054 (2016).
14. C. Y. Cho, C. C. Pu, Y. F. Chen, and K. W. Su, "Energy scale-up and mode-quality enhancement of the LED-pumped Nd:YAG Q-switched laser achieving a millijoule green pulse," Opt. Lett. **44**(13), 3202 (2019).
15. B. Villars, E. Steven Hill, and C. G. Durfee, "Design and development of a high-power LED-pumped Ce:Nd:YAG laser," Opt. Lett. **40**(13), 3049 (2015).
16. A. Barbet, A. Paul, T. Gallinelli, F. Balembois, J.-P. Blanchot, S. Forget, S. Chénais, F. Druon, and P. Georges, "Light-emitting diode pumped luminescent concentrators: a new opportunity for low-cost solid-state lasers," Optica **3**(5), 465 (2016).
17. P. Pichon, A. Barbet, J.-P. Blanchot, F. Druon, F. Balembois, and P. Georges, "LED-pumped alexandrite laser oscillator and amplifier," Opt. Lett. **42**(20), 4191 (2017).
18. P. Pichon, A. Barbet, J.-P. Blanchot, F. Druon, F. Balembois, and P. Georges, "Light-emitting diodes: a new paradigm for Ti:sapphire pumping," Optica **5**(10), 1236 (2018).
19. P. Pichon, F. Druon, J.-P. Blanchot, F. Balembois, and P. Georges, "LED-pumped passively Q-switched Cr:LiSAF laser," Opt. Lett. **43**(18), 4489 (2018).
20. L. Hu, D. Sun, J. Luo, H. Zhang, X. Zhao, C. Quan, Z. Han, K. Dong, M. Cheng, and S. Yin, "Effect of Er3 + concentration on spectral characteristic and 2.79 µm laser performance of Er:YSGG crystal," J. Lumin. **226**, 117502 (2020).
21. D. K. G. De Boer and L. Haenen, "Extraction optics for high lumen density sources," J. Eur. Opt. Soc.-Rapid Publ. **15**(1), 8 (2019).
22. L. Lopez, P. Pichon, P. Loiseau, B. Viana, R. Mahiou, F. Druon, P. Georges, and F. Balembois, "Ce:LYSO, from scintillator to solid-state lighting as a blue luminescent concentrator," Sci. Rep. **13**(1), 7199 (2023).
23. R. H. Wilson, K. P. Nadeau, F. B. Jaworski, B. J. Tromberg, and A. J. Durkin, "Review of short-wave infrared spectroscopy and imaging methods for biological tissue characterization," J. Biomed. Opt **20**(3), 030901 (2015).
24. A. M. Smith, M. C. Mancini, and S. Nie, "Second window for in vivo imaging," Nat. Nanotechnol. **4**(11), 710–711 (2009).